Available online at www.sciencedirect.com
SCIENCE DIRECT
Journal of Molecular Catalysis A: Chemical 252 (2006) 63–69
JOURNAL OF MOLECULAR CATALYSIS A: CHEMICAL
www.elsevier.com/locate/molcata

Characteristic and electrocatalytic behavior of ruthenium Prussian blue analogue film in strongly acidic media

Annamalai Senthil Kumar [1], Jyh-Myng Zen *

Department of Chemistry, National Chung Hsing University, Taichung 402, Taiwan

Received 17 August 2005; received in revised form 1 February 2006; accepted 2 February 2006
Available online 23 March 2006

Abstract

The remarkable stability of ruthenium Prussian blue analogue (designated as RuOx–PB) in strongly acidic media and for the enzymeless electrocatalytic oxidation of glucose was demonstrated in this study. The RuOx–PB combinative film neither dissolves nor denatures in concentrated acids, such as $HClO_4$, HCl, H_2SO_4, and HNO_3, investigated in this study. The catalytic response was found to directly proportional to $[H^+]$. Such features are unique since neither RuOx- nor PB-based compounds are effective for direct carbohydrate oxidation in acidic media. The RuOx–PB film showed a highly reversible redox peak at ~1.2 V in 5 M $HClO_4$ as a result of the fast proton-coupled electron transfer behavior of high valent ruthenium intermediate, $Ru^{VII/VI}$. The formation of internal multiple-hydrogen bond as well as the generation of the $\rangle Ru^{VII}$=O species in strongly acidic media were proposed to play a key role in this feature. The RuOx–PB holds high potential for use in catalytic oxidation, corrosion protection, biofuel cell, etc.

Keywords: Ruthenium oxide; Prussian blue; Strong acid; Glucose; Electrocatalysis

1. Introduction

Prussian blue (PB) and its analogues are mixed-valent bimetallic zeolite type of supramolecular compounds with polymeric internal structure and have been used for numerous applications [1–6]. Ruthenium Prussian blue analogue (–$RuRu(CN)_6$–) was reported to perform excellent electrocatalytic activity towards the oxidation of alcohols, thiols, aldehyde, amide, methanol, and insulin in ~pH 2 solution in the presence of alkaline metal ions [7–16]. The –$RuRu(CN)_6$– film is believed to possess the combined characteristics of ruthenium oxide (RuOx) and PB and is thus referred to as RuOx–PB henceforth. Recently our studies on this material reveal a peculiar behavior of unusual stabilization of electrogenerated high-valent intermediate, $\rangle Ru^{VII}$=O, in pH 2 media [17–19]. The performance in glucose catalytic oxidation reaction was further demonstrated, as it is important in biological and biochemical systems as well as in bioenergy technology. Note that even though glucose oxidation is a thermodynamically allowed reaction, it is kinetically unfavored on most solid electrodes (including RuOx) in acidic media.

Here we report an interesting electrocatalytic behavior with stable characteristics of the RuOx–PB in strongly acidic media (e.g., 5 M $HClO_4$). Both the $\rangle Ru^{VII}$=O stabilization effect and the catalytic performance were substantially improved with the increase in $[H^+]$. It is well known that the classical PB analogues are soluble even in diluted acid condition [20], and so is the ruthenium oxy/hydroxide material under acidic condition of $[H^+] \cong 1$ M. The concentrated acid-assisted stabilization and catalytic activity of the RuOx–PB combinative analogue is thus a breakthrough and novel to the mixed-valent bimetallic material chemistry and holds high potential of use for catalytic oxidation, corrosion protection, biofuel cell, etc.

2. Experimental

Cyclic voltammetric (CV) experiments were carried out using a CHI 406 electrochemical workstation (Austin, TX, USA). The three-electrode system consists of either a glassy carbon electrode (GCE) or a screen-printed carbon electrode (SPE) as a working electrode, an Ag/AgCl reference electrode (RE-5,

* Corresponding author. Fax: +886 4 22854007.
E-mail address: jmzen@dragon.nchu.edu.tw (J.-M. Zen).
[1] Present address: Department of Chemistry, Nara Women's University, Nara, Japan.

1381-1169/$ – see front matter © 2006 Elsevier B.V. All rights reserved.
doi:10.1016/j.molcata.2006.02.038

BAS), and a platinum auxiliary electrode. Since dissolved oxygen did not interfere with the working system, no deaeration was performed in the present study. The simplified equation of $E_{RHE} = [(E_{Ag/AgCl} + 0.06pH) + E^{o}_{Ag/AgCl}(0.22)]$ was used for converting the potential between $E_{Ag/AgCl}$ and E_{RHE} (RHE, reversible hydrogen electrode) [17].

Prior to the modification, a GCE was polished and sonicated in dilute 0.1 M HNO_3 for ~3 min. The indium tin oxide (ITO) electrode was first washed with acetone and then sonicated in 0.1 M HNO_3 for ~5 min. All working electrodes were equilibrated for 10 continuous CV cycles at respective base electrolyte with a scan rate (ν) of 50 mV/s followed by washing with copious amount of distilled water. Supporting electrolytes used in the work include concentrated HNO_3 (14.4 M), H_2SO_4 (18.0 M), HCl (12.1 M), $HClO_4$ (11.6, 5, 0.5, and 0.01 M), and pH 2 (0.01 M HCl + 0.1 M KCl) solution. The RuOx–PB was prepared by a potential cycling method (from −0.5 to 1.25 V at $\nu = 50$ mV/s, $n = 20$) using 1 mM $RuCl_3$ + 1 mM $Ru(CN)_6^{3-}$ solution in different base electrolytes. To reduce the charging current of the Nafion/RuO_2 modified SPE, RuO_2 powder was pretreated at 500 °C for 6 h in a muffle furnace [21]. Then 75 mg/ml RuO_2 powder was mixed with 5 wt.% Nafion solution followed by sonication at room temperature for 5 min. Finally, 5 μl of the above solution was dip-coated onto a clean SPE surface and allowed to dry for ~30 min in air.

Nafion (5 wt.% in lower aliphatic alcohols), ruthenium trichloride hydrate, ruthenium oxide, ITO, and potassium hexacyano ruthenate^{II} were purchased from Aldrich. D(+)glucose was bought from Sigma. SPE (0.07 cm^2) was obtained from Zensor R&D (Taichung, Taiwan). Other chemicals employed were of analytical grade and used without any purification. Aqueous solutions were prepared from doubly distilled deionized water.

3. Results and discussion

3.1. Electrochemical properties of the RuOx–PB

So far, almost all classical PB and its related analogues were prepared and stabilized in the presence of alkali metal ions (e.g., KCl). In this work, according to the formation of RuOx–PB in both pure acid and acid + alkali metal ion conditions, the RuOx–PB shows a H^+-dependent and alkali metal ion-independent stability. Fig. 1 compares typical responses to the formation process of RuOx–PB in 0.01 M $HClO_4$ (A) and conventional 0.01 M, pH 2 KCl/HCl medium (B) at a scan rate of 50 mV/s for 20 cycles. As can be seen, the responses are qualitatively similar except that the latter case shows a relatively higher current response. In classical PB electrochemical behavior, alkaline metal ions (especially K^+) are necessary to maintaining the electrical neutrality and further stabilizing the face center cubic structure as shown below [1].

$$KFe^{III}[Fe^{2+}(CN)_6] + K^+ + e^- = K_2Fe^{II}[Fe^{2+}(CN)_6]$$

$$KFe^{III}[Fe^{2+}(CN)_6] = Fe^{III}Fe^{3+}(CN)_6 + K^+ + e^-$$

In the above equations, $Fe^{III/II}$ and $Fe^{3+/2+}$ correspond to high spin and low spin of iron, respectively. It is unusual to observe

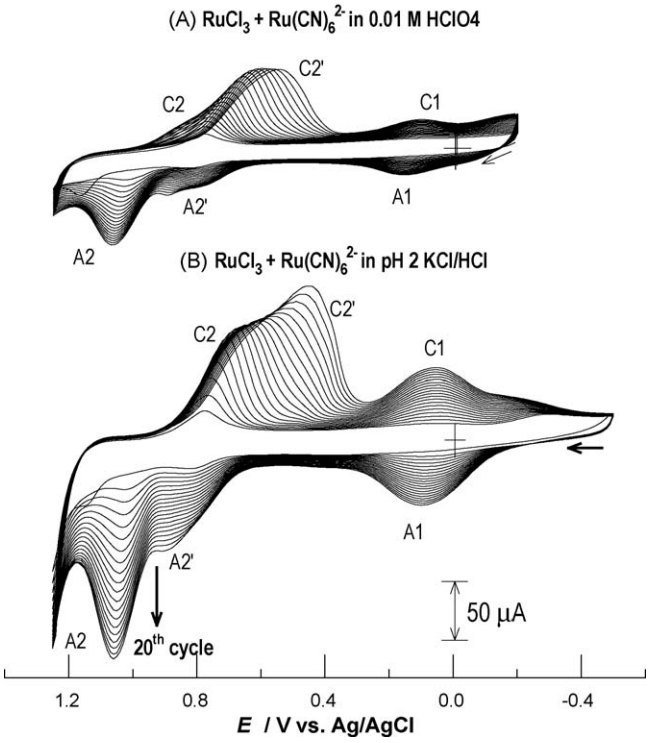

Fig. 1. Cyclic voltammetric responses for the formation of RuOx–PB films on GCE in different supporting electrolytes with 1 mM each of $RuCl_3 + Ru(CN)_6^{2-}$ at a scan rate of 50 mV/s.

such a redox behavior at the RuOx–PB in the absence of alkaline metal ions. Interestingly, the behavior is also true in other strongly acidic media, such as HCl, H_2SO_4, and H_3PO_4. Because of a wide potential window of $HClO_4$ medium, it was chosen in all subsequent studies.

As shown in Fig. 1, the three redox couples centered at ~0.1, ~0.8, and ~1.0 V versus Ag/AgCl correspond to the redox peak responses of A1/C1, A2′/C2′, and A2/C2, respectively, in the RuOx–PB matrix. As is the case with PB, A1/C1 and A2′/C2′ are the electron transfer reactions of high spin nude metal ions (–CN–$Ru^{III/II}$–) and low spin cyanometallate ions (–$Ru^{III/II}(CN)_6$–), respectively [7–11,13–15]. Different assignment, however, were reported for the A2/C2 redox couple by various groups. For example, either –$Ru^{VI/IV}$O– or –Ru^{VI}(=O)$_2$–/–(OH)Ru^{V}(=O)– redox species were assigned by Cataldi et al. [10,13,14]; Gorski and Cox [11] suggested the existence of (–O–)$_2Ru^{IV}(OH)_2(OH_2)_2$/(–O–)$_2Ru^{VI}(OH)_4$ at 1.0 V versus Ag|AgCl in pH 2 solution; Loetanantawong et al. [22] reported a tetracycline electrocatalysis at 1.10 V versus Ag|AgCl in pH 1 solution from the $Ru^{IV/III}$ redox couple; Chen et al. [23] reported the electrocatalytic oxidations of dopamine, thiols, and alcohols in pH 1.5 solution at ~1.0 V versus Ag|AgCl as $Ru^{IV}O_2/Ru^{III}{}_2O_3$ state.

In order to justify the A2/C2 assignment, our group has adopted an indirect method to investigate the exact nature of the Ru redox group within RuOx–PB in pH 2 solution by conducting selective oxidation reactions with well-stabilized redox organic probes [17,18]. This is similar to earlier RuOx-based electrocatalytic studies in which the higher ⟩$Ru^{VII/VI}$=O redox couple

was responsible for selective glucose oxidation in alkaline pH (pH > 12) and the lower redox state $Ru^{VI/IV}$ for formaldehyde oxidation in a wide pH range of 1–14. We found the existence of the high-valent $\rangle Ru^{VII/VI}$=O redox state at 1.0 V versus Ag|AgCl unusually in the RuOx–PB film in pH 2 solution. Parallel ex situ X-ray photoelectron spectroscopic (XPS) studies with the RuOx–PB film prepared by potentiostatic technique at 1.1 V versus Ag|AgCl (where the $\rangle Ru^{VII}$=O species can be electrogenerated) prove the existence of oxy (–O–), hydroxy (–OH) and aqua ($–OH_2$) functioned $\rangle Ru^{VII}$=O traces within the RuOx–PB film [17]. Although the precise nature of the RuOx–PB structure is not known, the available physicochemical and electrochemical evidence suggests that basic RuOx–PB network contains combination of (i) –C≡N–, (ii) –Ru–O–Ru–, and (iii) strong hydrogen bonding linkages [17,18]. Note that classical PB is made up purely with cyano blocks; while RuOx consists of –Ru–O–Ru– and hydrogen bonding [1].

According to the CV of Fig. 1A, a relatively weak nucleation response of the A1/C1 redox process indicates a limited role of the alkali–metal ion to stabilize the network structure in the RuOx–PB. As an alternative, the proton intercalation at A2/C2 and A2′/C2′ is expected to be essential for the network stability and hence for the redox catalysis in the acidic condition. This is also reflected in the fact that some of the redox active sites of the RuOx–PB are highly deficient in proton. Based on these results, the electrochemical activity of RuOx–PB in strongly acidic media should be related to –Ru–O–Ru– and strong hydrogen bonding rather than the –C≡N– (i.e., A1/C1) linkages (Fig. 2).

Regarding the Ru^{VII} oxidation state, perruthenate ion (RuO_4^-) is a well-known inorganic compound with a solution phase redox potential of 1.35–1.45 V versus RHE [24–26]. Burke et al. concluded that, in strong alkaline condition, the RuO_4^- species can exist in the RuO_2-coated electrode at a redox potential close to the solution phase RuO_4^- ions [27]. Later development suggested that the solid phase RuO_4^- consists of the ruthenium oxo and hydroxo species [21,28–30]. Both RuO_4^- and oxy–/hydroxy– $\rangle Ru^{VII}$=O inorganic analogues were unstable and can disproportionately decompose (DDP) to lower oxidation states of $Ru^{IV}O_2$ and RuO_3 in pH < 12 solution [26,27]. Fig. 3 illustrates the RuO_4^-/RuO_4^{2-} redox characteristics and selective glucose oxidation with a conventional RuO_2 electrode in 0.1 M NaOH solution. As can be seen, a well-defined, intense, and reversible redox couple was obtained at 0.45 V versus Ag|AgCl (equivalent to 1.49 V versus RHE) corresponding to RuO_4^-/RuO_4^{2-}. In agreement with the reported standard redox potentials, the other Ru redox transitions of RuO_4^{2-}/RuO_2 and RuO_2/Ru_2O_3 appeared with relatively weaker signals at ~0 V versus Ag|AgCl (1.06 V versus RHE) and −0.6 V versus Ag|AgCl (0.45 V versus RHE), respectively [31]. In the presence of glucose, a clear electrocatalytic signal ($E_{1/2}$ = 0.45 V vs Ag/AgCl) was noticed originating from the oxidation state RuO_4^-/RuO_4^{2-}. This result thus rules out the possibility of glucose oxidation by lower oxidation states of RuO_4^{2-}/RuO_2 and RuO_2/Ru_2O_3 using conventional RuO_2-based electrodes.

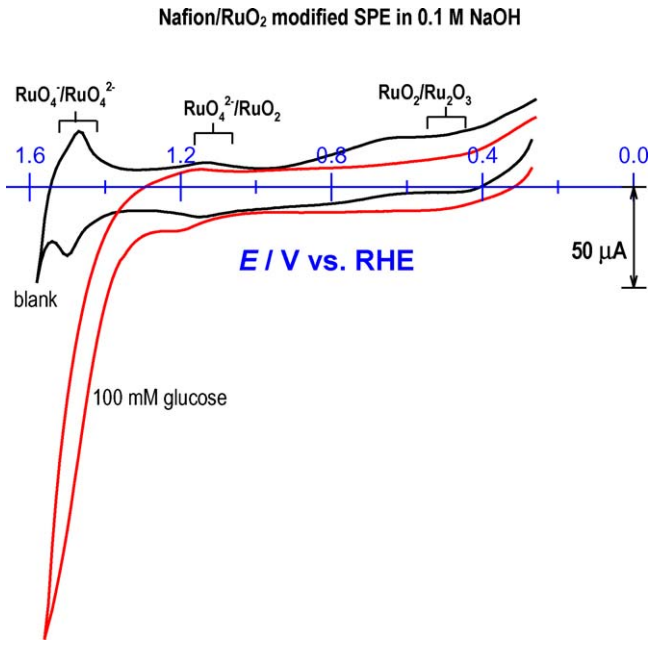

Fig. 3. Cyclic voltammetric responses of a Nafion/RuO_2 modified SPE without/with 100 mM glucose in 0.1 M NaOH at a scan rate of 10 mV/s. The parenthesis corresponds to the respective Ru redox transitions in the CV graph.

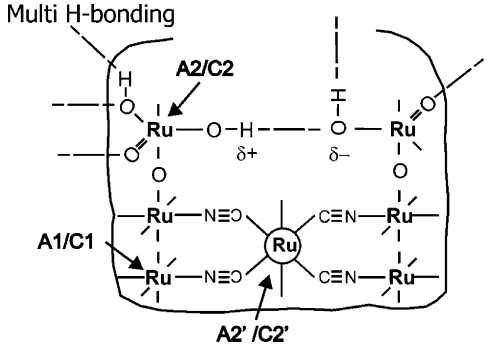

Fig. 2. Schematic representation of the RuOx–PB film with –Ru–CN–Ru–, –Ru–O–Ru– and multi-hydrogen bonding sites proposed in this work.

3.2. *Catalysis for carbohydrates oxidation in acidic solution*

The obvious effect of the acidity towards the glucose oxidation at the RuOx–PB film can be seen in Fig. 4A. Both A2/C2 and A2′/C2′ peak responses are markedly altered as the concentration of proton varied. This is not the case with the A1/C1 in base electrolyte. Upon increasing the acidity, both A1/C1 and A2′/C2′ peaks start to decrease with an increase in the reversibility of the A2/C2 redox couple. As the acidity increases to 5 M $HClO_4$, the A2/C2 peak leads to a perfect reversible nature in couple with the disappearance of both A1/C1 and A2′/C2′ peaks. Note that these characteristics are similar to the surface bound RuO_4^-/RuO_4^{2-} species observed with a RuO_2 electrode in alkaline condition as shown in Fig. 3. Presumably with a facile proton-coupled electron transfer redox behavior of the electrogenerated $\rangle Ru^{VII/VI}$=O, the peak potential separation (ΔE_p) is

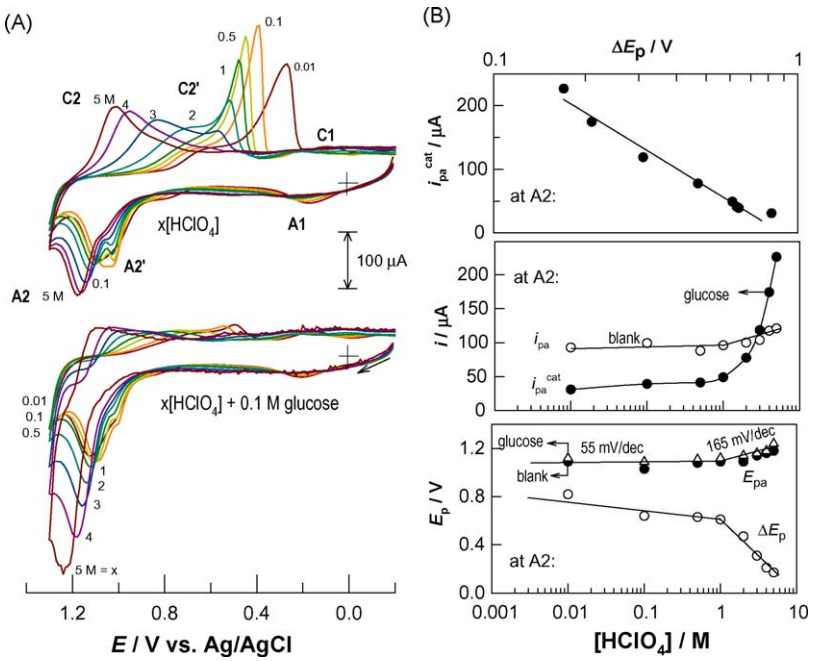

Fig. 4. (A) Cyclic voltammetric responses of the RuOx–PB in various [$HClO_4$] with/without 100 mM glucose at $\nu = 50$ mV/s. (B) E_p vs. log[$HClO_4$], i_{pa} vs. log[$HClO_4$], and i_{pa}^{cat} vs. ΔE_p plots.

close to 0 mV. Most importantly, this observation is new and novel to the RuOx–PB redox chemistry.

Detailed electrocatalytic responses of the RuOx–PB film in the presence of glucose are studied next. As can be seen in Fig. 4B, the i_{pa}^{cat} (i.e., $i_{pa}^{glucose} - i_{pa}^{blank}$) responses are relatively weak in 0.01–1 M $HClO_4$; while a steep increase in the i_{pa}^{cat} response is noticed in strongly acidic media of 1–5 M $HClO_4$. The increase in the i_{pa}^{cat} value was ~200 times as the concentration of $HClO_4$ increased from 0.01 to 5 M. Fig. 4B also shows various plots applied to analyze the feature of the RuOx–PB and its catalytic behavior against [$HClO_4$]. First, the plot of E_{pa} versus [H^+] yields a slope of 55 mV/dec in 0.01–1 M $HClO_4$ and increases by ~3 times (165 mV/dec) in 1–5 M $HClO_4$. This is an interesting result as it denotes different proton-coupled electron-transfer/charge-transfer mechanism of ($1H^+$, $1e^-$) and ($3H^+$, $1e^-$) in weakly and strongly acidic media, respectively. Note that since the RuOx–PB contains three mixed valence electron-transfer processes, it is highly difficult to isolate single peak effect of A2/C2 from the overall system. In dilute [H^+] solution, the cathodic peak signals (i_{pc} and E_{pc}) were masked or coupled with counter reduction peak currents (Fig. 4A). Since the A2/C2 redox couple showed reasonable reversible peak characteristics, we took the anodic peak potential, E_{pa}, as a reference to the pH effect. The following speculative reaction mechanism for the A2/C2 redox couple is proposed for the PB–RuOx under weakly and strongly acidic conditions at an applied potential of 1.2 V versus Ag/AgCl.

The functional ligands with the Ru species are similar to the earlier assignment on RuO_2 and RuOx–PB [11,28]. In fact, our own XPS data also supports the observation with strong hydrogen bonding effect [17].

As reported earlier, surface functional group and its H^+ and/or OH^- interaction is a key to the RuOx redox transition [21,27–30]. In concentrated acids, most of the surface functional groups should get protonated and are thus capable of forming strong multi-hydrogen bonding (both inter and intra) in the network. The phenomena can be understood easily as illustrated in Fig. 5. As is the case with the gear function in machine, either OH^- or H^+ can act as a control gear to convert the Ru-redox transition without rupturing the basic network under its corresponding working potentials. In the functional model, a higher slope base was drawn indicating the necessity of strong alkaline condition with high potential to achieve the high-valent $Ru^{VII/VI}$ species in the RuOx system. Note that Nernstian response is not expected for pure/ideal metal oxides because H^+ and OH^- are not lattice ions in principle. The observation of pH-dependent behavior (Nernstian type) implies a specific role of the surface bound H^+/OH^- ions in the redox transition. The discussion also validates the hydrogen bonding effect within the functional group together with the –Ru–O–Ru– and –C=N– linkages to protect the framework from the DDP reaction in this work. Since the secondary hydrogen bonding effect was reported to control and organize the DNA and RNA supramolecular structures [32], it is

Step-1: slope = 55 mV/pH

$$\boxed{\text{PB}}\text{-(-O-)}_2\text{Ru}^{\text{VI}}\text{O}^-(\text{OH})_3 + 1\text{H}^+ \rightarrow \text{PB-(-O-)}_2\text{Ru}^{\text{VII}}(=\text{O})(\text{O}^-)(\text{OH})_2 + \text{H}_2\text{O} + 1\text{e}^-$$

Step-2: slope = 165 mV/pH

$$\boxed{\text{PB}}\text{-(-O-)}_2\text{Ru}^{\text{VI}}\text{O}^-(\text{OH})_3 + 3\text{H}^+ \rightarrow \text{PB-(-O-)}_2\text{Ru}^{\text{VII}}(=\text{O})(\text{OH}_2{}^*)_2 + \text{H}_2\text{O} + 1\text{e}^-$$

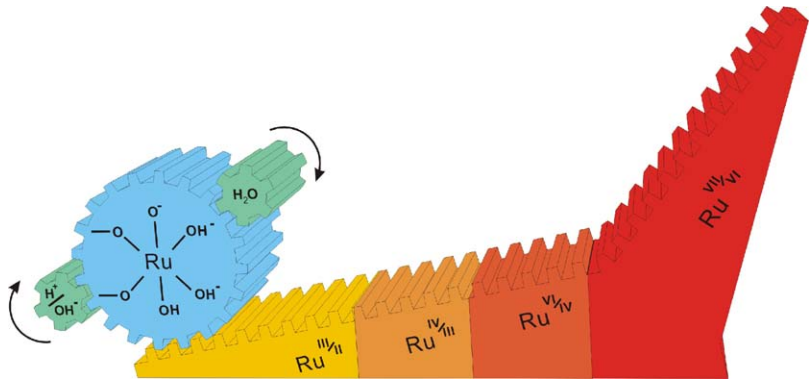

Fig. 5. A gear cartoon picture represents the surface functional group assisted RuOx redox transition mechanism. The high-valent $Ru^{VII/VI}$ redox state can be operated only at strong alkaline condition; while in acidic condition Ru^{VII} roll-down to lower oxidation states of $Ru^{IV}O_2$ and $Ru^{VI}O_3$.

thus expected that some unusual configuration with non-ideal PB structures may exist in the RuOx–PB. Of course, further characterization is necessary to confirming the real structure. Nevertheless, considering the fact that classical PB analogues are highly soluble even in dilute acid [20], numerous practical applications can be readily imagined with this new catalytic system.

Effect of the scan rate (ν) on the glucose catalysis was finally investigated in concentrated 5 M $HClO_4$ solution. The catalytic current values were found to regularly increase against $\nu^{1/2}$ up to 200 mV/s indicating a diffusion controlled mechanism. Current function, $i_f = i^{cat}/\nu^{1/2}$ (i^{cat}: baseline uncorrected catalytic current) was calculated by normalizing the catalytic current against $\nu^{1/2}$. As can be seen in Fig. 6, a parabolic type of response where the i_f value showed a maximum at slower ν was obtained. This is a typical example of the "EC" coupled chemical reaction with the reaction mechanism as shown in Scheme 1.

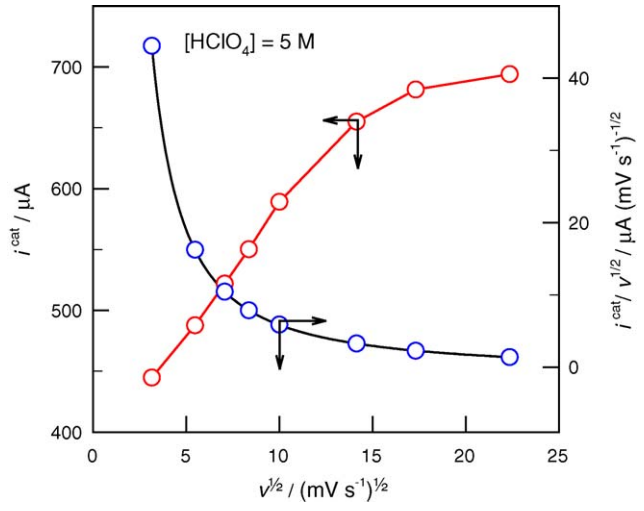

Fig. 6. Plots of catalytic current (left) and current function (right) against square root of scan rate for catalytic glucose (100 mM) oxidation reaction at the RuOx–PB in 5 M $HClO_4$.

3.3. Stability in strongly acidic media

Fig. 7A shows typical CV responses of the RuOx–PB upon increasing concentration of glucose in 5 M $HClO_4$ at $\nu = 10$ mV/s. The catalytic response is linear up to 100 mM with sensitivity (I_s) of 1.01 μA/mM. As shown in inset Fig. 7, the I_s value is ~4 times as large as the case of $[HClO_4] = 0.5$ M.

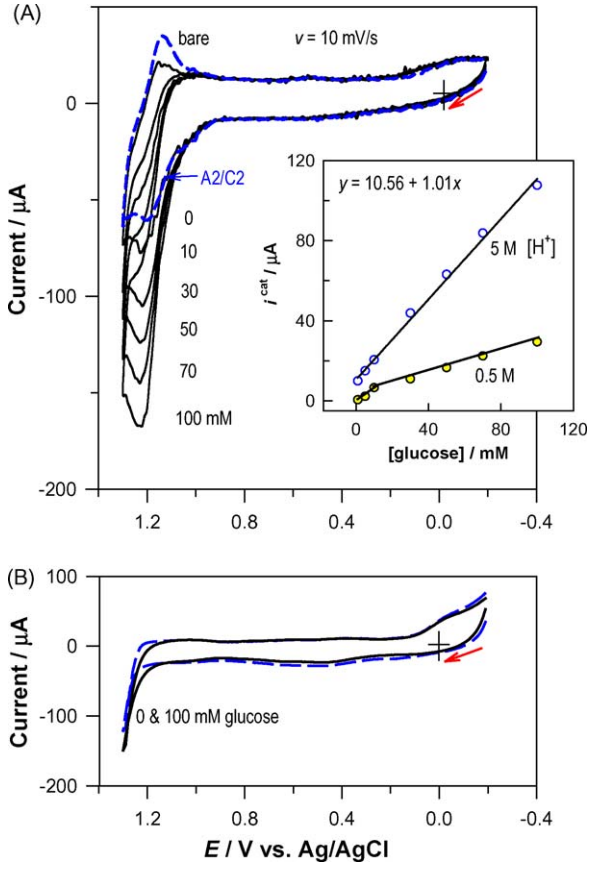

Fig. 7. Cyclic voltammetric responses of increasing [glucose] at (A) RuOx–PB and (B) Nafion/RuO_2 modified SPE in 5 M $HClO_4$ ($\nu = 10$ mV/s). Inset figure shows the plots for the catalytic current response obtained from 5 and 0.5 M $HClO_4$ against [glucose] at the RuOx–PB.

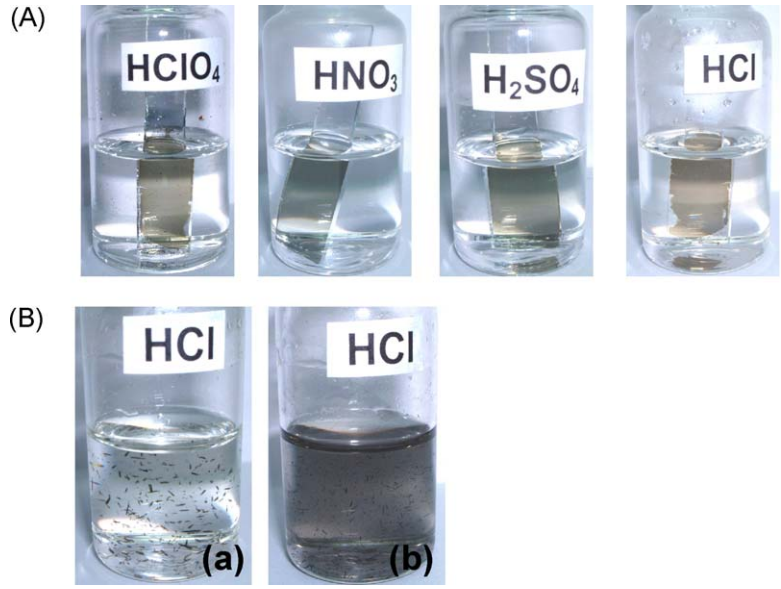

Fig. 8. Pictures of (A) RuOx–PB/ITO electrodes in different concentrated acids and (B) insoluble RuO-PB microcrystals (peel off from RuOx–PB/ITO by a spatula) in the absence (a) and presence (b) of ~10 mg RuO_2 in concentrated HCl.

Parallel experiment with a RuO_2-modified electrode failed to give such an activity and catalytic response in strongly acidic media (Fig. 7B). Long-term stability of the RuOx–PB film was further checked by continuous cycling in $HClO_4$ solution for ~30 min. Excellent stability was observed especially in strongly acidic condition of $[HClO_4] > 1$ M. The RuOx–PB was found to degrade slowly in $[HClO_4] < 1$ M media with the A2 peak current decreased by ~35% in 0.01 M $HClO_4$ after continuous cycling for 30 min. This is also true even in the presence of alkaline metal ions.

To further test the stability, an RuOx–PB modified ITO electrode was thus prepared and immersed in various concentrated acid solutions of $HClO_4$ (11.6 M), HNO_3 (14.4 M), H_2SO_4 (18.0 M), and HCl (12.1 M). As can be seen in Fig. 8A, the RuOx–PB films were highly stable in all concentrated acids.

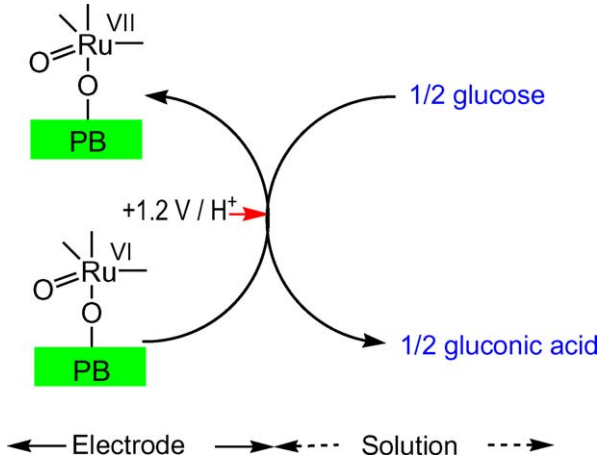

Scheme 1. Conceptional representation for the proton-coupled glucose oxidation at the electrogenerated $\rangle Ru^{VII}{=}O$ intermediate site within the RuOx–PB in strongly acidic media. A minimal structure of the network confined with $-Ru^{VII/VI}{=}O$ active site was presented.

When ~10 mg of commercially available RuO_2 powder sample was mixed with a RuOx–PB microparticle containing concentrated HCl solution, black color appeared, clearly indicating the high solubility of the RuO_2 powder (Fig. 8B). The RuOx–PB, on the other hand, is stable with a clear solution under the same concentrated acid condition. Note again that classical PB film starts to dissolve even in <1 M of acid solution [20].

To test the repeatability of the RuOx–PB preparation procedure, four RuOx–PB films were prepared individually. A very small RSD value of <3% for glucose oxidation as a model indicates that the preparation method reported in this study is highly repeatable. Overall, the characteristics of the RuOx–PB material in concentrated acid solution open a new research direction in the development of corrosion protection, catalysis and biofuel cell, etc.

4. Conclusions

A ruthenium Prussian blue analogue (RuOx–PB) film has been demonstrated to substantially mediate glucose oxidation in strongly acidic media. Unlike regular PB redox behavior, the RuOx–PB shows a reversible proton-coupled electron-transfer response corresponding to the $\rangle Ru^{VII/VI}{=}O$ redox transition at 5 M $HClO_4$. In contrast to classical PB electrodes, the high-valent Ru species holds a perfect surface character without any disproportionation–decomposition reaction. A bare RuO_2-based electrode is unable to stabilize the high-valent $\rangle Ru^{VII}{=}O$ species in $pH < 12$ solutions. With the stabilization of high-valent $\rangle Ru^{VII}{=}O$ species, glucose is oxidized by an EC type of mechanism. The sensitivity in the determination of glucose using the RuOx–PB film increases by ~4 times as the concentration of $HClO_4$ increases from 0.5 to 5 M. Considering the anti-corrosion behavior in concentrated acids, the RuOx–PB material can be useful for a variety of applications and further work is in progress in our laboratory.

Acknowledgment

The authors gratefully acknowledge financial support from the National Science Council of Taiwan.

References

[1] K. Itaya, I. Uchida, V.D. Neff, Acc. Chem. Res. 19 (1986) 162.
[2] O. Kahn, Nature 399 (1999) 21.
[3] B.P. Jelle, G. Hagen, J. Electrochem. Soc. 140 (1993) 3560.
[4] D.M. de Longchamp, P.T. Hammond, Adv. Funct. Mater. 14 (2004) 224.
[5] A.A. Karyakin, Electroanalysis 13 (2001) 813.
[6] J.-M. Zen, P.-Y. Chen, A.S. Kumar, Anal. Chem. 75 (2003) 6017.
[7] J.A. Cox, P.J. Kulesza, Anal. Chem. 56 (1984) 1021.
[8] J.A. Cox, R.K. Jaworski, P.J. Kulesza, Electroanalysis 3 (1991) 869.
[9] P.J. Kulesza, M. Bandoch, J. Electroanal. Chem. 323 (1992) 131.
[10] T.R.I. Cataldi, D. Centonze, A. Guerrieri, Anal. Chem. 67 (1995) 101.
[11] W. Gorski, J.A. Cox, J. Electroanal. Chem. 389 (1995) 123.
[12] L. Hyang, H. Shen, M.A. Atkinson, R.T. Kennedy, Proc. Natl. Acad. Sci. U.S.A. 92 (1995) 9608.
[13] T.R.I. Cataldi, D. Centonze, E. Desimoni, V. Forastiero, Anal. Chim. Acta 310 (1995) 257.
[14] T.R.I. Cataldi, A.M. Salvi, D. Centonze, L. Sabbatini, J. Electroanal. Chem. 406 (1996) 91.
[15] P.J. Kulesza, B. Grzybowska, M.A. Malik, M. Chojak, K. Miecznikowski, J. Electroanal. Chem. 512 (2001) 110.
[16] J.A. Cox, L. Cheng, in: A. Brajter-Toth, J.Q. Chambers (Eds.), Electroanalytical Methods for Biological Materials, Marcel Dekker, New York, 2002, pp. 417–438.
[17] A.S. Kumar, J.-M. Zen, ChemPhysChem 5 (2004) 1227.
[18] A.S. Kumar, J.-M. Zen, Electroanalysis 16 (2004) 1211.
[19] A.S. Kumar, P.-Y. Chen, S.-H. Chien, J.-M. Zen, Electroanalysis 17 (2005) 210.
[20] L.F. Schneemeyer, S.E. Spengler, D.W. Murphy, Inorg. Chem. 24 (1985) 3044.
[21] A.S. Kumar, K.C. Pillai, J. Solid State Electrochem. 4 (2000) 408, and references therein.
[22] B. Loetanantawong, C. Suracheep, M. Somasundrum, W. Surareungchai, Anal. Chem. 76 (2004) 2266.
[23] S.-M. Chen, M.-F. Lu, K.-C. Lin, J. Electroanal. Chem. 579 (2005) 163.
[24] R.E. Connick, C.R. Hurley, J. Am. Chem. Soc. 74 (1952) 5012.
[25] D. Silverman, H.A. Levy, J. Am. Chem. Soc. 79 (1954) 3317.
[26] K.W. Lam, K.E. Johnson, D.G. Lee, J. Electrochem. Soc. 125 (1978) 1069.
[27] L.D. Burke, J.F. Healy, J. Electroanal. Chem. 124 (1981) 327.
[28] M.E.G. Lyons, L.D. Burke, J. Chem. Soc., Faraday Trans. 1 (83) (1987) 299.
[29] Yu.E. Roginskaya, I.D. Belova, B.Sh. Galyamov, Yu.M. Popkov, D.S. Zakhar, Russ. Electrochem. 23 (1987) 1145.
[30] M.E.G. Lyons, C.A. Fitzgerald, M.R. Smyth, Analyst 119 (1994) 855.
[31] A.J. Bard, R. Parsons, J. Jordan, Standard Potentials in Aqueous Solutions, IUPAC, Marcel Dekker, New York, 1983, p. 413.
[32] C.R. Calladine, H.R. Drew, Understanding DNA, The Molecule & How It Works, Academic Press Inc., San Diego, CA, 1992.